3. Experimental

3.1 Basic principles of SFM

3.1.1 Operating principle

The operation principle of a scanning probe microscope (SPM) is based on the detection of the position of a soft cantilever-type spring with a sharp tip mounted at its end. The forces acting on the tip after it has approached the sample surface cause a deflection of the cantilever according, in a first approximation, to the Hooke's law. This bending is controlled by a feedback loop, which regulates the vertical position of the tip with respect to the sample surface. By keeping the deflection constant while scanning the sample, a three-dimensional map of the surface topography can be obtained.

Usually, as shown in Figure 2, the vertical tip position is read using a laser beam, which is reflected by the end of the cantilever and detected using a differential optical converter. The arrows in Figure **2** emphasize the "trajectory" of the feedback loop: SFM tip, laser beam, detector, controller, Z scanner and sample. The key point of the system is the fact that the feedback loop contains the "tip-sample interaction" element.

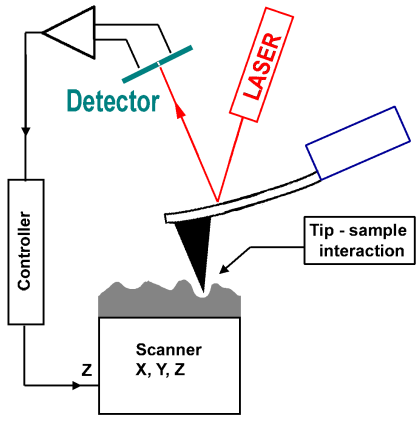

Figure 2 Principle of the SPM-based techniques.

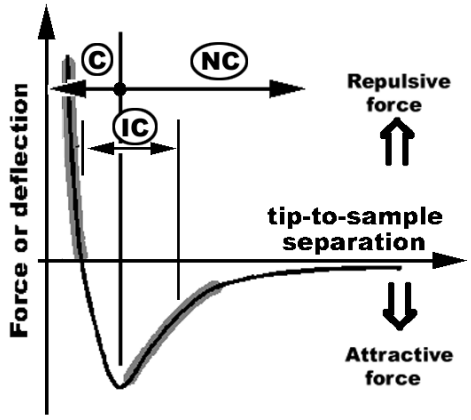

Figure 3 Force versus tip-sample separation. "C", "NC", and "IC" denote the contact, non-contact, and intermittent contact regions of the curve.

There are two main modes of operation that determine the type of interaction between the SFM tip and the sample: contact and non-contact. In contact mode, the probing tip senses the short-range repulsive forces exerted by the surface. The interaction between tip and sample can be estimated plotting the cantilever deflection against the elevation above the surface of the Z scanner, the so-called *force–distance* curve. The shape of a typical force curve is shown in Figure 3. A tip approaching the surface first senses the long-range forces. This region of the curve is used in non-contact mode imaging. The forces are usually Van der Waals forces, but any other type of interaction between the SPM tip and the surface of the sample should be

included, depending on the given tip and sample. For instance, if the SPM tip has a magnetic moment, the long-range attractive and repulsive magnetic forces are sensed and the magnetic domain structure at the surface can be visualized. Further approaching the tip, the interaction force becomes repulsive and the cantilever is deflected in the opposite direction. This region is used in the contact mode technique.

Another important type of measurement used in this work is directly related to the detection of lateral forces acting on the SPM tip. In principle, this is done in the contact mode of operation. With the lateral force technique, the probe is scanned perpendicularly to the long axis of the cantilever. The torsion of the cantilever supporting the probe will increase or decrease, depending on the frictional characteristics of the surface (a greater torsion results from an increased friction).

3.1.2 Topography imaging with SFM

As mentioned above, to image the topography of a sample the tiny forces between a sharp tip and the sample surface are utilized. In contact mode (cf. Figure 3), the tip elevation is adjusted via the feedback loop in order to follow the surface height using the deflection signal, which is in fact the cantilever bending caused by repulsive forces.

For example let us suppose that the tip is scanned at a constant altitude above a flat surface. The tip being in contact, there is always a repulsive force that bends the cantilever, with a constant value called “setpoint”. If there are no variations in the cantilever bending, the tip is scanned at the same altitude, and the tip height representing the topographic data render a flat surface. If the tip arrives at a protuberance of the surface, the cantilever feels a higher contact force and bends more than before. The deflection signal increases, and as a consequence, the feedback controller raises up the tip until the deflection signal equals the setpoint again. If the tip encounters a pit during its scan then the feedback process will lower the tip elevation because the contact force (and therefore the deflection signal) is decreased in this case. The elevation of the tip therefore reflects the surface topography and is used to image it. In fact the principle explained above is used for imaging in all modes of operation.

In the non-contact mode, the tip feels the attractive forces exerted by the surface and the setpoint value in this case represents a bending in the opposite direction than in the repulsive mode. If the tip meets a surface protrusion, the attractive force increases and the feedback control system raises up the tip until the attractive force takes the setpoint value. This mode of operation is quite difficult to achieve, and very easy to destabilize. The amount of force available to be used is much smaller than in the repulsive mode (see Figure 3).

The operating modes described up to now were static. In the dynamic modes the same principle is used, but the signal that is monitored by the feedback loop is the amplitude of the cantilever vibration, induced mechanically with a piezoelectric oscillator (at the cantilever resonance for a maximum sensitivity).

In the dynamic non-contact mode the amplitude of the cantilever oscillation increases if the surface has an elevation and the feedback control adjusts the tip elevation until the amplitude reaches the setpoint value again. This mode is an improvement of the non-contact static mode, with an increased sensitivity.

Another mode of topographic imaging is the intermittent-contact mode (also called “tapping” mode), which is an improvement of the contact mode, developed to decrease the

interaction of the tip with the surface. The cantilever with the tip is oscillated at its resonance frequency and the height is adjusted so that the tip touches the sample surface only for a short period of time. If the tip encounters an elevation, the oscillation amplitude will decrease and the feedback control raises up the cantilever until the oscillation amplitude reaches the initial value.

3.2 Probing ferroelectric domains by SFM

SFM-based methods of ferroelectric domain imaging make use of basic properties of ferroelectrics, namely of their elastic or piezoelectric behavior and/or of the presence of surface charges, associated with the permanent built-in electric polarization. In very specific cases, the topography caused by the domain structure is sufficient to deduce the direction of the spontaneous polarization. A static surface charge, proportional to the normal component of the polarization, can be detected when the microscope is operated in the non-contact (attractive) mode. By monitoring the piezoelectric vibration of the ferroelectric sample caused by an external AC voltage, the domain structure can be visualized in the SFM piezoresponse mode, when the probing tip is in contact with the sample.

3.2.1 Domain imaging with SFM contact and non-contact static modes

Before explaining the proper domain imaging modes, the historically first attempts to investigate domains with SFM should be reviewed. These techniques are termed “static” because no dynamic interaction (mechanic or electrostatic) between the SFM probing tip and the ferroelectric domains is involved during the imaging process. True atomic resolution was achieved on flat surfaces of different materials [11], even under ambient conditions [12].

Domain imaging in the topography mode

Morphological domain contrast can result as a consequence of different phenomena, according to the specific material properties. Topographic features of the sample surface can be imaged either in contact or in non-contact mode, the interpretation of the domain images does not depend on the type of interaction used to obtain the topographic information. Therefore the results considered in this section were obtained either in contact, non-contact or intermittent contact modes of operation. The very high vertical resolution of SFM proved to be useful to investigate the surface morphology and to relate it to the ferroelectric domain structure. It should be mentioned that true atomic resolution was achieved in the topography mode at the surface of ferroelectric crystals [13,35].

A particular example is the case of triglycine sulfate (TGS), which is one of the most frequently studied ferroelectric crystals. It was shown that steps form at domain boundaries during the crystal cleavage due to the structural difference between the positively and negatively charged ends of the domains [14,15,16]. Bluhm et al. [15,16], using the SFM topography mode, have found that the step height is different on the opposite cleavage faces. The difference was explained by the different relative shift of atom positions at the surface of opposite domains. Due to the different etching behavior of positive and negative domains in TGS [17] topographic imaging of this crystal was used for the identification of the domain polarity in a number of studies [14,18,19,20,21]. In the case of the TGS crystal, the cleavage plane is perpendicular to the polar axis, therefore the imaged surface was thought to interact

electrostatically with the conductive or non-conductive SFM tip. However, ferroelectric domains have been imaged even if the cleavage plane of the crystal is parallel to the polar axis, as in the case of K_2ZnCl_4 [22]. In the latter case, the topographic contrast was proven to be due solely to the transverse piezoelectric deformation of the ferroelectric domains.

In case of the tetragonal phase of perovskite ferroelectrics, the polarization vector can be aligned along six directions, which are equivalent in the cubic paraelectric phase. Along the polarization direction the unit cell is slightly elongated leading to the tetragonal distortion of the unit cell. In a (001) single crystal plate, the domains with the polarization perpendicular to the plane of the plate are called *c*-domains and the domains with the polarization in the plane of the plate are called *a*-domains. In the regions between the *a*- and *c*-domains (the so-called 90° domain walls) the tetragonality causes a distortion of the lattice, which results in a tilt angle between the surfaces of the two domains. Figure 1 shows a schematic cross-section view of such a plate containing *a*- and *c*-domains. The tilt angle between the surfaces of the two types of domains can be estimated from the tetragonal distortion as $\theta = 2arctg(c/a) - 90° \approx 0.6°$. This allows the deduction of the domain structure of ferroelectric perovskites from the topography of the crystal surface, taking into account the criteria presented in Sect. 2.3. Using these assumptions, domain structures were successfully deducd and analyzed from SFM topographic images in $BaTiO_3$ [23,24,25], $PbTiO_3$ [26,27] crystals and also in $PbTiO_3$ ceramic [28] and epitaxial PZT (20/80) thin films [29]. Also, by applying pulse voltages to the SFM tip while scanning in contact mode, the domain structure could be modified by means of nucleation and growth of opposite *c*-domains [30,31,32]. In these studies it was necessary to mount the ferroelectric crystal on an electrode in order to apply electric fields to the sample. The observation of different *c*-domains using the topography mode of SFM was possible *via* static piezoelectric deformation caused by the application of a small DC voltage between the tip and a bottom electrode.

Domain imaging in the friction mode

It was assumed that ferroelectric domains may induce a lateral force contrast *via* electrostatic tip-sample interaction. During the movement of a non-conducting tip across the ferroelectric sample surface, a certain amount of charges accumulates [31] or an electric dipole forms [33] on the probing tip. The moving charged tip senses different lateral forces above ferroelectric domains with opposite orientations. The same experiment performed with a grounded conducting tip (which does not retain any charge) did not reveal any domain contrast. As a consequence, it was thought that this proves the electrostatic nature of the interaction. The observed reversal of domain contrast for opposite scanning directions [19] supported the tribological effect to be present in the imaging mechanism.

Later on, however, it appeared that the ferroelectric domains can more likely induce a lateral force contrast due to the structural differences of the surfaces of oppositely polarized domains [34]. Bluhm et al. demonstrated for both guanidinium aluminum sulfate hexahydrate (GASH) and TGS crystals that the domain contrast in friction mode is not governed by electrostatic interaction between the tip and the surfaces. For the GASH surface, they found indeed a reversal of the domain contrast for forward and backward scan directions, but the magnitude of friction forces did not show opposite signs for opposite scanning directions, as it should. For the case of TGS, the results were more difficult to interpret, since the lateral force was found to be highly anisotropic, i.e. a strong dependence of the domain pattern on the

scanning angle was found. Moreover, if the electrostatic interaction would be responsible for the domain contrast, then the latter should reverse when the surface is scanned first with positive and then with negative voltages applied to the tip. In the experiments performed in inert atmosphere switching the voltage from –10V to +10V resulted only in a change of the offset of the friction signal. Therefore, even if the electrostatic interaction cannot be completely ruled out, it does not entirely explain the mechanism of domain contrast in the friction mode of SFM.

It should also be noted that SFM friction imaging is a technique very sensitive to the properties of the tip-to-sample interface and therefore special care has to be taken when interpreting the tribological contrast as revealing ferroelectric domains. Adhesion layers, wetting, contamination, interfacial and surface chemistry can easily obscure the electrostatic interaction. The method works very well on freshly cleaved surfaces, if the cleavage plane is perpendicular to the polar axis. This is the case for GASH and TGS for which this method, although controversial, was successful [35]. A comparative characterization of the *a*- and *c*-domains in epitaxial $PbTiO_3$ and $BaTiO_3$ thin films on MgO (100) substrates was also possible, revealing the smaller transformation strain and larger compressive stress in $BaTiO_3$ at the Curie temperature [36].

In conclusion, it should be emphasized that there are obvious limitations on the applicability of the SFM topographic and friction modes for the imaging of ferroelectric domains. These methods can be applied only for crystals with cleavage planes, since any treatment of the surface during sample preparation inevitably eliminates the subnanometer structure of morphological steps associated with the ferroelectric domain structure. Also, domain imaging by inducing static piezoelectric strain with a DC voltage is almost impossible to perform if the surface has a roughness of several nanometers, comparable with the deformation induced by a reasonable DC voltage of 10 V.

3.2.2 SFM dynamic non-contact modes

As mentioned in Sect. 3.1.1, the SFM system can probe not only the surface topography, but any type of interaction between the SFM tip and the sample. Since the feedback loop keeps the amplitude of the cantilever oscillation constant, any modification of the interaction force will lead to a variation of both the feedback and output signals. Therefore, if a non-topography-related interaction is governing the feedback loop, the topography can not be monitored anymore, but only the sources of the probed interaction. This inconvenience is usually ruled out simply, by scanning over the same line twice, with two different feedback signals, one dominated by the topography and the other by the non-topographic interaction. In the case of ferroelectric domain imaging, the electrostatic interaction between the probing tip and the electric field at the sample surface controls the feedback loop.

Domain imaging in the dynamic non-contact mode

In the SFM dynamic non-contact mode of operation, the cantilever is vibrating near its resonance frequency at a distance of 5 nm to 100 nm above the sample surface, being driven by a piezoelectric oscillator. The topographic imaging principle, which was only simply described in Sect. 3.1.2, is explained in terms of a shift in the resonance frequency due to the tip-to-

sample interaction. As the tip is scanned over the surface, the resonance frequency of the cantilever is modified in function of the distance between tip and sample surface. A change of the resonance frequency results in a change of the response amplitude of the cantilever at the driving frequency. Using a lock-in technique the amplitude of the oscillation is detected and is used as an input for the feedback loop to adjust the *z*-position of the tip so that the elevation above the surface is maintained constant.

In the case of the ferroelectric samples, an additional shift of the resonance frequency appears due to the electrostatic interaction between the biased conductive tip and the electric field at the surface. When the vibrating tip enters a region with a non-homogeneous electrostatic field, the effective spring constant of the cantilever changes and this results in an extra shift of its resonance frequency. An image of the electric field gradient is therefore obtained in the dynamic mode [19]. Moreover, it was pointed out that only the component normal to the cantilever axis affects the resonance frequency [37] and usually it is assumed that, for most of the geometries, only the z-component of the gradient is important. Using this method, the lowest detectable force gradient was estimated by Lüthi et al. [19] to be 10^{-3} N/m.

The first experiments using the electrostatic interaction to control the feedback loop of an SFM were performed to detect localized charges deposited on insulators by Stern et al. [38] at IBM. A study of ferroelectric domains using the non-contact dynamic mode, was first reported only one year later by the same group [39]. Since an electric field gradient above a flat ferroelectric surface can exist near the domain walls, this method proved to be sensitive enough to image ferroelectric domain walls at a polished surface of the ferroelectric-ferroelastic material $Gd_2(MoO_4)_3$.

It should be mentioned that the image contrast depends essentially on the external bias voltage applied to the probing tip and on the tip material. By varying the bias voltage, the contrast of domain wall boundaries can be eliminated and a contrast between opposite domains can be observed [19]. A similar approach can provide a detection mechanism for previously written ferroelectric domains [40].

The voltage modulated non-contact mode

In order to improve the sensitivity of the method described above and to distinguish the signal given by the surface charge from other possible sources of the force gradient, it was suggested to apply a small AC voltage between the bottom electrode and the probing tip [39]. The frequency of this additional voltage should be far away from the cantilever resonance, in order to avoid any interference with the mechanical oscillation of the cantilever used in the feedback loop. The AC voltage results in alternating positive and negative charges on the tip. The tip-sample electrostatic force will thus also be periodic, causing a synchronous cantilever vibration, which can be detected using a lock-in technique with a much better signal-to-noise ratio than in the case of a DC bias. By monitoring the first harmonic signal, information about the surface charge distribution can be obtained. Another advantage of this method is that it is sensitive to the charge only and allows the determination of its sign.

This technique was further improved for surface potential imaging by using the AC-voltage-driven oscillation as a feedback signal to adjust the DC bias. Since the procedure is very similar to the one used by Lord Kelvin to determine the surface potential, the method was denominated Kelvin Probe Microscopy (KPM) [11,41,42,43].

A serious drawback of the techniques described in this section is that they are sensitive not only to the electric field but also to the other interactions between the tip and the surface (such as the Van der Waals forces). Therefore the data recorded should be deconvoluted to obtain the information on the ferroelectric domain structure [20]. If the experiments are performed under ambient conditions, the capillary force due to the adsorbed water layer should also be taken into account, since it would reduce the cantilever amplitude. Also, as it is well known, the electric field gradient strongly depends on the curvature of the surface. As a result, in the case of domains of irregular shape and corrugated surface topography, the electric field gradient signal is in fact a superposition of topography, damping on the surface, Van der Waals forces and the "true" signal, and accordingly it might be very difficult to interpret the images.

3.2.3 SFM dynamic contact mode

Also called voltage-modulated SFM, or piezoresponse-SFM, this method has proven to be the most suitable method to *study* and to *control* the ferroelectric domain structure at the nanometer scale. The main advantage is that it simultaneously allows the modification and detection of the ferroelectric polarization on a local level.

Evolution of piezoresponse-SFM

This technique was first used in 1991* by H. Birk et al. [44] who measured the piezoelectric coefficient in a ferroelectric copolymer of vinylidene fluoride and trifluorethylene using a scanning tunneling microscope (STM). The copolymer film was sandwiched between an aluminum layer and a 20 nm thick gold electrode, both used for applying voltages to the film and to enable the STM operation. Piezoelectric surface oscillations were induced using an AC voltage (10 V, 20 Hz) applied between the electrodes and detected with a lock-in amplifier connected to the feedback signal of the STM. When operating in constant current mode, the STM tip is kept at a constant distance from the sample and the feedback signal represents the vertical position of the sample surface. This new method proved to be useful to measure the local longitudinal piezoelectric coefficient and to show its hysteresis. One year later, the same group [45] succeeded in polarizing and imaging micron-sized ferroelectric domains in copolymer films without the top electrode, using atomic force microscopy combined with a lock-in technique, by detecting the local vibrations of the sample surface.

The first application of piezoresponse-SFM to the study of ferroelectric films of lead zirconate titanate (PZT) was reported in 1994 by Franke et al. [46]. One year later the signals involved in this technique were analytically calculated using a simple one-dimensional model [47,48]. The characterization of domain reversal in PZT films by recording *local hysteresis loops* was first reported by Hidaka et al. [49]. Systematic studies of domain dynamics, retention and fatigue effects have been carried out for thin films of PZT-based materials [50,51]. Also, investigations of ferroelectric domains at the surface of barium titanate ($BaTiO_3$), triglycine sulfate (TGS) and potassium trihydrogen phosphate (KTP) bulk single crystals were successfully performed [52,53,54]. The well-known domain structure of $BaTiO_3$ facilitated the validation and development of the detection of in-plane ferroelectric domains [55] leading to the mapping of all three components of polarization at the ferroelectric surfaces [56].

* to the best knowledge of the author.

However, the first results concerning the observation of the ferroelectric domain structure of other thin film materials than PZT were only reported in 1998 for $SrBi_2Ta_2O_9$ by Gruverman and Ikeda [57], and in 1999 for $BaBi_4Ti_4O_{15}$ and $Bi_4Ti_3O_{12}$ by our group [58,59,60].

Principle of piezoresponse-SFM

The piezoresponse-SFM technique is based on the converse piezoelectric effect, which is a linear coupling between the electrical and mechanical properties of a material. Since all ferroelectrics exhibit piezoelectricity, an electric field applied to a ferroelectric sample results in changes of its dimensions. Moreover, in most ferroelectric materials the piezoelectric effect can be interpreted as the electrostriction phenomenon biased by the spontaneous polarization [8] leading to the conclusion that the piezoelectric coefficient and the spontaneous polarization are directly related (see Sect. 2.2).

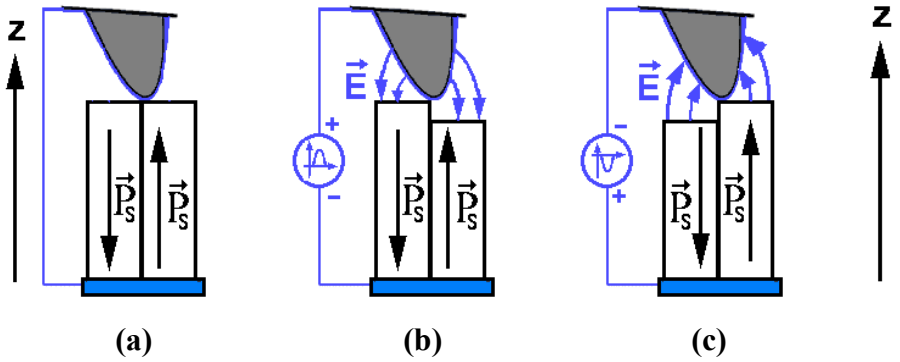

Figure 4 Principle of piezoresponse SFM **(a)** No topographic contrast if no voltage is applied. **(b)** A change in thickness occurs for a positive voltage applied to the tip (or during the positive half periods of an AC voltage). **(c)** Opposite thickness changes for a negative voltage (or during the negative half periods).

To detect the polarization orientation the SFM tip is used as a top electrode, which can be moved over the sample surface. To illustrate the imaging mechanism let us consider the simplified example circuit shown in Figure 4, with the ferroelectric sample sandwiched between a bottom electrode and the conductive SFM tip. Also let us consider two ferroelectric domains having opposite orientations of polarization, perpendicular to the sample surface. In Figure 4a no voltage is applied between the electrodes and the two ferroelectric domains have the same dimension in z-direction, only governed by the spontaneous strain which is the same for the two domains (since it has a quadratic dependence on polarization, as shown in Sect. 2.2). When a voltage is applied to the tip, the electric field generated in the sample causes the domains with the polarization parallel to the field to extend and the domains with opposite polarization to contract. The images (b) and (c) in Figure 4 illustrate the z-deformation of the domains when a positive, respectively negative voltage with respect to the bottom electrode is applied to the tip. To describe, in a first approximation, the electric field-induced displacements of the sample surface, we consider the following assumptions:

- The surface displacement is equal to the entire piezoelectric displacement induced in the sample; that is, the back surface of the ferroelectric is fixed [61]. Any non-zero compliance of the bottom electrode would reduce the surface displacements.

- The electric field is uniform inside the ferroelectric sample, in the region underneath the SFM tip.
- The positive z-axis is as shown in Figure 4a, i.e. it is oriented from the bottom electrode towards the SFM tip.
- The voltages are given with respect to the bottom electrode.
- The spontaneous polarization is normal to the film plane.

Using the constitutive equations for the piezoelectric effect (Eq. 5a in Sect. 2.2) and the above assumptions, the following relation can be obtained (X = 0 was assumed):

$$\Delta z = -d^* V \qquad \textit{Eq. 11}$$

where $\begin{cases} d^* = d_{33} \quad for \quad positive\ domains, \quad P_z > 0 \\ d^* = -d_{33} \quad for \quad negative\ domains, \quad P_z < 0 \end{cases}$

The negative sign derives from the negative electric field caused by the application of a positive voltage to the tip; that results in a negative displacement of the surface when a positive voltage is applied to a positive domain.

A usual numeric value for the piezoelectric coefficient, d_{33} = 50 pm/V and applied voltage 4 V (a value limited by the coercive field of the film), result in a piezoelectric deformation of 0.2 nm which has to be detected (Eq. 11). This value is very close to the lower resolution of a usual SFM, and such a displacement can be very easily obscured by topographic features of 5 nm to 10 nm. Therefore, a DC voltage method is not suitable to monitor the ferroelectric domains on rough surfaces. Using an AC method combined with lock-in detection considerably improves the signal-to-noise ratio. By replacing the voltage in Eq. 11 with $V = V_{AC}\sin(\omega t)$ the surface movements induced underneath the tip are given by:

$$\Delta z(t) = \begin{cases} \Delta z^+(t) = -d_{33} V_{AC} \sin(\omega t), & P_z > 0 \\ \Delta z^-(t) = d_{33} V_{AC} \sin(\omega t), & P_z < 0 \end{cases} \quad \text{, or}$$

$$\Delta z(t) = \Delta z_0 \sin(\omega t + \Phi), \qquad \textit{Eq. 12}$$

Where the superscript $^+$ and $^-$ denote positive and negative domains, respectively, and:

$$\begin{cases} \Delta z_0 = d_{33} V_{AC} & \\ \Phi = \pi & \text{for positive domains, and} \\ \Phi = 0 & \text{for negative domains.} \end{cases} \qquad \textit{Eq. 13}$$

Therefore, opposite orientations of polarization along the z-axis cause the sample surface to vibrate out of phase under a small AC voltage. The name "*voltage-modulated SFM*" of this method originates from the fact that during the scanning process, the SFM tip passes across different ferroelectric domains which modulate the carrier of information (the AC oscillation in this case) with their mechanical response, according to the local polarization orientation. Figure 5 illustrates the demodulation process.

The detection of the surface vibrations (or demodulation of the information on the polarization state) can be performed using a standard lock-in technique, as described below. The vertical position of the SFM tip (or its deflection) is usually monitored in SFM techniques using a laser beam, which is reflected by the cantilever on which the SFM tip is mounted. Using an optical detector the cantilever bending is converted into an electrical signal (the deflection

signal) and is further processed by the SFM controller. In piezoresponse-SFM, the deflection signal also contains the induced oscillations of the sample surface transmitted to the tip-cantilever. These electrical oscillations can be simply extracted from the global deflection signal using a lock-in amplifier. The lock-in detection rules out any other harmonic components of the deflection signal and the piezoelectric oscillations are in this way separated from the topography. The signal detected by the lock-in amplifier is usually referred to as the *piezoresponse* signal [29] and is directly related to the amplitude and phase of the surface vibration *via* the detector sensitivity δ:

$$v_\omega = \delta \Delta z_0 \cos(\Phi) \qquad \textit{Eq. 14}$$

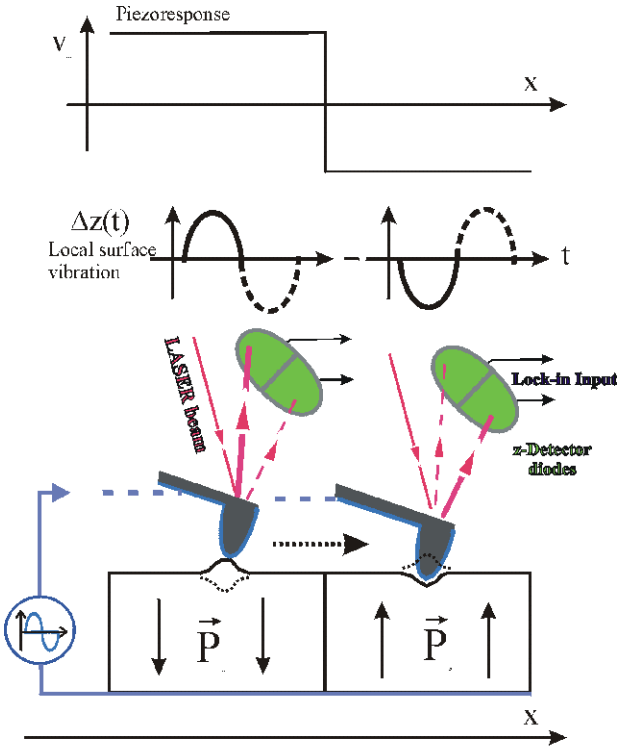

Figure 5 Demodulation of the information on the polarization state from the piezoresponse signal. The latter is modulated by the spatial variations of the piezoelectric coefficient.

The piezoresponse signal expressed in Eq. 14 contains an information about the polarization orientation of the area under the SFM tip *via* the phase shift Φ and also about the magnitude of the piezoelectric coefficient, provided that the phase factor can take only the two values indicated in Eq. 13 over the entire sample surface. This signal can be detected using a simple, single phase, lock-in amplifier. Using a dual lock-in amplifier it is possible to measure simultaneously the amplitude and the phase of the signal, therefore to study other phenomena such as the local piezoelectric losses. However, special care has to be taken regarding the analysis and interpretation of the phase signal.

Detection of the in-plane polarization by piezoresponse-SFM

Using the converse piezoelectric effect it is also possible to detect an in-plane component of the polarization vector (parallel to the sample surface). The basic principle of this detection consists

in the existence of piezoelectric shear deformations (Figure 6). If the polarization vector is perpendicular to the electric field, there is no piezoelectric deformation along the field direction, but a shear strain appears in the ferroelectric, leading to displacements of the sample surface parallel to itself, along the polarization direction. In the case of piezoresponse-SFM the in-plane displacements of the surface are transferred *via* friction to the SFM tip as lateral movements. The component of these movements perpendicular to the cantilever axis induces a torsion of the cantilever end, which can be detected using the capability of the SFM to measure the cantilever torsion.

The shear deformation depends on the polarization orientation and for the case of tetragonal perovskites with extended electrodes and the geometry illustrated in Figure 6 ($\vec{P} \| \vec{c} \| x, \vec{E} \| -\vec{a} \| -z$, and *cantilever axis* $\| \vec{b} \| y$, with *xyz* the coordinate system, and *abc* the crystallographic axes of the ferroelectric crystal) can be expressed as:

$$x_5 = -d^{**} E_z \qquad \textit{Eq. 15}$$

$$\text{where} \begin{cases} d^{**} = d_{15} \quad for \quad positive\ domains, \quad P_x > 0 \\ d^{**} = -d_{15} \quad for \quad negative\ domains, \quad P_x < 0 \end{cases}$$

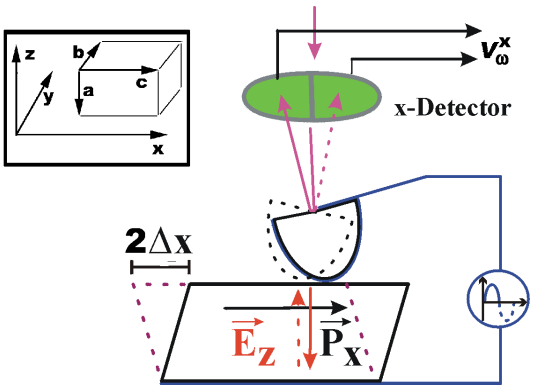

Figure 6 Detection of in-plane polarization. The inset shows the choice of the coordinate system and the crystallographic orientation of the ferroelectric crystal (the cantilever axis is parallel to the y-axis).

As in the case of detection of the domains with out-of-plane polarization, an AC field induces in-plane oscillations phase shifted by 180° in regions with opposite orientations of polarization.

$$\Delta x(t) = \Delta x_0 \sin(\omega t + \Phi), \qquad \textit{Eq. 16}$$

$$\text{where} \begin{cases} \Phi = \pi \ for \ positive\ domains, P_x > 0 \\ \Phi = 0 \ for \ negative\ domains, P_x < 0 \end{cases}$$

The surface vibrations described by Eq. 16 induce torsional oscillations of the cantilever with the same frequency. Due to the complex nature of the friction interaction it is difficult to describe them quantitatively. However, the phase shift of the oscillations above antiparallel domains describes the latter correctly, as it will be demonstrated in the analysis of the first

harmonic signals presented in Sect. 4.1. Therefore, in the case of in-plane detection the piezoresponse signal has a similar form as Eq. 14:

$$v_{\omega}^{x} = C\cos(\Phi)$$

where the constant C contains the detector sensitivity, the friction transmission factor, and the amplitude of the shear piezoelectric displacements.

It should be noted that a similar shear deformation is present along both the x-and y-axes. However, due to the cantilever asymmetry, domains having polarization along the y-axis can be recorded only by physically rotating the sample by 90°.

Two important features of the shear-piezoresponse signal should be mentioned. The first one is that the amplitude and phase only very weakly depends on the scan speed and does not depend on the scan direction. As it is well known for the friction (lateral force) technique, the deflection signal of the cantilever torsion increases almost linearly with the scan speed and reverses the sign when the scan direction changes. This is a normal behavior, since the friction torque is reversed for opposite scanning directions. However, the phase of the (additional) in-plane piezoresponse signal is not affected by the change in sign of the global friction signal.

Another important characteristic of the in-plane piezoresponse detection is that the signal is present even if the SFM tip is fixed on the surface. In the friction technique, only the dynamic friction coefficient between the SFM tip and the surface has been used, to date, for surface characterization. Estimation or comparison of static friction coefficients would require very tiny and accurate lateral movements of the scanner, a possibility which has not yet been implemented by SPM manufacturers. That is, when the tip is fixed on the surface, the static friction signal has no significant meaning. In spite of this fact, the amplitude of the shear piezoresponse signal is the same if the tip is stationary or scanned with a low speed.

The two features mentioned above are proofs that the origin of the first harmonic signal extracted from the friction signal is a real movement of the sample surface parallel to itself and that it is not picked-up from the circuitry of the electronic box. Moreover, by applying bias voltages to the tip it is possible in some situations to modify the polarization orientation of the in-plane domains, causing changes of the piezoresponse signal.

3.2.4 Theoretical approach to the tip-to-ferroelectric sample interactions

Understanding the tip-to-sample electrostatic interactions represents a key challenge in the field of electrostatic force microscopy (EFM). This comes from the fact that the electrostatic sensor has a complex shape: a cantilever with a conical or pyramid-shaped tip ending in a spherical apex. Since SFM is based on the detection of the cantilever movements, the models are focused on the description of the forces acting on the tip [62]. Several attempts to describe the conductive tip-dielectric system with or without a bottom electrode can be found in the literature. Mainly, the models are developed along three directions. In this section a brief description of each model will be given.

The layered capacitor model

If only the qualitative analysis of the phenomena is required, then the simplest approach consists in modeling the tip and the sample with the bottom electrode as a capacitor [47,48]. This

approach proved to be useful for the analysis of the signals implied in electrostatic [39,63] and Kelvin force microscopy [41,64,65].

In a first approximation, the volume under the tip-sample contact area can be considered as a capacitor composed of two layers (Figure 7). The upper layer with thickness h and permittivity ε_i represents the interface between the tip and the sample. The lower ferroelectric layer, which represents the sample itself, is described by the thickness t, the field-independent component of polarization P and the permittivity ε_f (which describes the linear component of polarization). In the case of non-contact EFM the upper dielectric is represented by the air gap, whereas for contact EFM, it can be a thin water layer adsorbed at the surface [66].

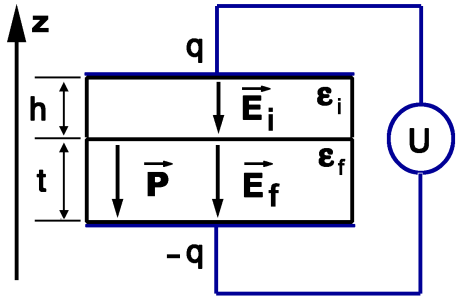

Figure 7 Simple layered capacitor model for the estimation of the deflection signals in EFM.

The electrostatic force (also called Maxwell stress force) acting on the tip can be easily found using Eq. 17, where the integral extends over the entire volume V of the capacitor. Since the normal component of the force acting on the tip is to be calculated, the derivation with respect to the tip elevation h has to be taken [47,48].

$$F^{el} = -\frac{\partial}{\partial h} W^{el} = -\frac{\partial}{\partial h}\left(\frac{1}{2}\int_V \vec{E}\cdot(\vec{D}-\vec{P})\, dV - qU \right) \qquad \textit{Eq. 17}$$

In the expression of the free energy, the term $-\vec{E}\cdot\vec{P}/2$ represents the energy density due to the fixed (spontaneous) polarization, and the term $-qU$ represents the energy supplied by the voltage source to the system. The force can be calculated using the system of equations given in Eq. 18 (for the designations see Figure 7).

$$\begin{cases} D = \varepsilon_i E_i = \varepsilon_f E_f + P \\ U = h\cdot E_i + t\cdot E_f \end{cases} \qquad \textit{Eq. 18}$$

In EFM experiments, the voltage applied to the tip has the form:

$$U = V_{DC} + V_{AC}\sin(\omega\tau) \qquad \textit{Eq. 19}$$

Considering that the cantilever deflection is proportional to the force *via* Hooke's law, the signals measured by a lock-in amplifier are directly proportional to the harmonic components of the force acting on the cantilever. These harmonic components can be calculated by solving the system Eq. 18 for the electric fields, introducing them in Eq. 17 and using Eq. 19. The result is presented in Eq. 20:

$$F = F_0 + F_\omega + F_{2\omega}, \quad \textit{where} \quad F_{k\omega} = \frac{2}{T}\int_0^T F(\tau)\sin(k\omega\tau)\, d\tau$$

$$\begin{cases} F_0 = -\alpha\left[\left(V_{DC} + \dfrac{P}{\varepsilon_f}t\right)^2 + \dfrac{1}{2}V_{AC}^2\right] \\ F_\omega = -\alpha\left(V_{DC} + \dfrac{P}{\varepsilon_f}t\right)V_{AC}\sin(\omega\tau) \\ F_{2\omega} = \dfrac{1}{4}\alpha V_{AC}^2 \sin\left(2\omega\tau + \dfrac{\pi}{2}\right) \end{cases} \qquad \textit{Eq. 20}$$

The parameter α is given in Eq. 21, where C represents the equivalent small signal capacitance of the system, and $T = 2\pi/\omega$ is the period of the AC voltage.

$$\alpha = \frac{S}{\varepsilon_i\left(\dfrac{t}{\varepsilon_f} + \dfrac{h}{\varepsilon_i}\right)^2} = -\frac{\partial C}{\partial h} \qquad \textit{Eq. 21}$$

Analyzing the spectral components of the electrostatic force (Eq. 20) it is possible to qualitatively explain the EFM signals, and also their relevance for ferroelectric domain imaging. A discussion of the first harmonic signals involved in voltage modulated SFM can be found in Sect. 4.1.

The method of image charges

Another approach to describe the tip-sample electrostatic interaction is to consider the tip as a conductive sphere above the surface and to solve the electrostatic problem "conductive sphere-dielectric layer-conductive plane". The principle of the technique, as proposed by Goto and Hane, is to successively perform electrical imaging using the following three models: A point charge and a dielectric plane, a point charge and a conductive plane, and a point charge and a conductive sphere [67]. The electrical imaging for these simple models is described in the literature [68]. The potential of the sphere is set to the value V, and the conductive plane is grounded (it is kept at potential zero). V represents the voltage applied to the tip with respect to the bottom electrode. The procedure for the technique is as follows: First, an initial charge q_0 (Figure 8) is placed at the center of the sphere.

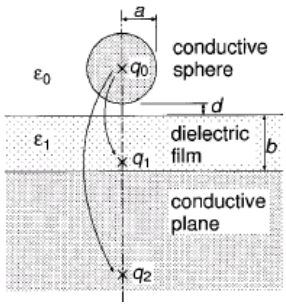

Figure 8 The method of image charges applied to EFM.

Next, two image charges, q_1 and q_2 (Figure 8), are created from q_0. The charges q_1 and q_2 are determined independently by the conventional charge image method [68] and are located in the

film and in the conductor, respectively. From each q_1 and q_2, two more image charges are created. The production of image charges is continued in a similar manner until the total charges in the sphere and plane converge. The tip–sample capacitance is given by dividing the total charges (real charges) by the tip–sample voltage V, and the force acting on the tip can be found in a similar manner as described in the previous paragraph.

A variant of this model, named *the equivalent charges model*, is based on the principle of distribution of equivalent charges, or the image method of equipotential surfaces. According to this principle, a conductor in electrostatic equilibrium can be replaced with a set of fictive charges inside it, in such a manner that one of the equipotential surfaces follows exactly the shape of the conductor [69]. Particularly, a conductive conical tip can be easily simulated with a distribution of charges placed on the cone axis. To solve the electrostatic problem of the real conductive tip and the dielectric sample, each of these charges has to be imaged as described above. This extension of the technique proved that the tip shape (pyramidal or conical for example) is not important, but that the lateral surface of the tip significantly contributes to the tip-sample capacitance for tip elevations higher than several nanometers above the sample surface.

The finite element method

A third approach to solve the electrostatic interaction between an SFM tip and a dielectric layer uses the finite element technique to compute exactly the potential and the electric field distribution. This method seems to be the most precise and also the most difficult. It requires an appropriate description of the geometry of the setup, which means that the respective shapes of the conductive tip and of the dielectric surface have to be mapped. To achieve a satisfactory spatial resolution for the solution without introducing errors due to the choice of the integrating domain, and also to maintain the mapping network at a reasonable size, Lanyi et al. [70] solved the problem for the cylindrical symmetry of a conical tip. Therefore a two-dimensional geometry can be applied with adequate boundary conditions for a restricted area around the tip apex to find out the equipotential surfaces and/or the electric field lines.

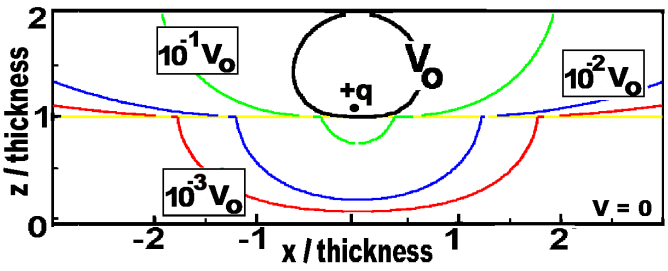

Figure 9 Equipotential lines of a point charge above a dielectric layer on a conductive plane, calculated with the method of image charges.

In this work a simplified variant of the image charges method was used to analyze the potential and electric field distribution induced by the SFM tip inside the sample. The theoretical calculations for an electrostatic system composed of a charge above a dielectric layer on a conductive plane are presented in Appendix A. The equipotential surfaces projected on the vertical plane containing the charge are shown in Figure 9. The finite element method for a simple geometry was also employed to qualitatively verify this result.

3.3 Piezoresponse-SFM setup

The experimental setup used in this work is schematically shown in Figure 10 and consists of a scanning probe microscope system, a lock-in amplifier, an AC voltage source, and a DC voltage supply. The scanning probe microscope (SPM) is a commercial Dimension 5000 microscope from Digital Instruments. For piezoresponse measurements the SFM was set to operate in contact mode, at a constant interaction force between the tip and the sample surface [71]. The value of the contact force depends on the spring constant of the cantilever, i.e. on its geometry and elastic properties.

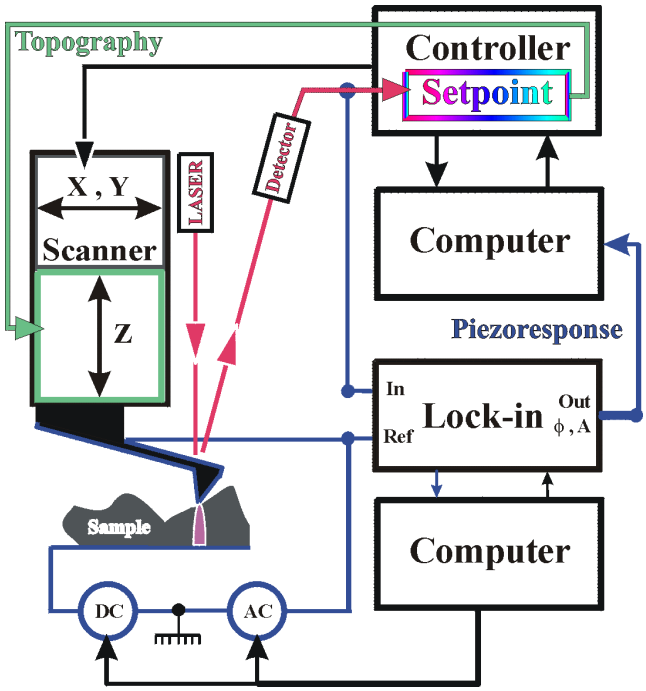

Figure 10 Experimental setup used for piezoresponse measurements.

In the constant force regime the feedback loop adjusts the vertical position by keeping a constant deflection of the cantilever so that not only the tip, but also the Z-scanner follows the local elevation of the sample surface. In this mode of operation the deflection signal, which represents the cantilever bending converted into an electrical signal by the optical detector, has a relative large constant value (of the order of 1 V, depending on the setting for the setpoint) over which small variations are superimposed (several mV). These variations are caused by the finite reaction time of the feedback loop and are proportional to the derivative of the feedback signal with respect to the time, i.e. if the scan speed is kept constant they represent the local slope of the sample surface along the scan direction.

For piezoresponse imaging, a small AC voltage has to be locally applied between the SFM tip and the bottom electrode of the sample, and the induced oscillations have to be detected, as described in Sect. 3.2.3. To extract the surface vibrations, a digital lock-in amplifier from EG&G Instruments, model 7260 was used. The signals were picked up from

intermediate processing stages* of the global deflection signal inside the electronic box controlling the SFM head. Since the lock-in internal noise limit is $2nV/\sqrt{Hz}$ [72] the measurement noise of $1.4\mu V/\sqrt{Hz}$ was determined by the electronic circuitry inside the SFM electronic box.

In most of the experiments, the internal oscillator of the lock-in amplifier was used as the AC source to induce the mechanical oscillations detected. The choice of the amplitude and frequency of the testing AC voltage depends on the specific experimental conditions. These conditions include two contradictory aspects:

- The AC amplitude has to be as small as possible, for a "non-destructive" testing, i.e. no switching of the ferroelectric polarization underneath the tip must be caused by the AC voltage. This implies that the amplitude has to be lower than the local coercive voltage of the ferroelectric domain, which may be different for each grain and even for each domain within the same ferroelectric crystallite [58]. As predicted by Gruverman et al. [29] and proven experimentally by our group [73], the occurrence of a polarization switching under the tip (with the frequency of the AC testing voltage) leads to a decrease of the piezoresponse signal and therefore makes the interpretation of piezoresponse data more difficult.

- To enhance the signal-to-noise ratio, the testing voltage has to be as high as possible in order to get a high amplitude of the mechanical vibration and thus a high piezoresponse signal. The main source of noise during the acquisition of the piezoresponse images is the global deflection signal itself, from which the first harmonic signal is extracted. The deflection signal, which is used by the SFM system as a feedback to maintain a constant force between tip and sample, is proportional to the scanning speed and to the derivative of the surface height with respect to the scan direction.

For samples with a high roughness, the deflection signal exhibits very sharp high peaks. These fast variations of the deflection signal may have harmonic components with the same frequency as the AC testing voltage and also amplitudes comparable with the piezoresponse signal. This noise may be overcome by using a low scanning speed and a high frequency probing voltage. However, this leads to a long recording time for the acquisition of the image. This is clearly demonstrated in the experiment illustrated in Figure 11, where the signals involved in piezoresponse imaging of a $Bi_4Ti_3O_{12}$ grain are shown for two different scanning speeds. The topography signal of a grain of $Bi_4Ti_3O_{12}$ divided into two ferroelectric domains was not influenced by changing the scan speed from 1 μm/s to 0.2 μm/s, but the deflection and piezoresponse signals show considerable reduction of noise.

The frequency of the testing signal has to be chosen far from any possible perturbing oscillations that may appear in the system, such as the resonance frequencies of the cantilever. Depending on sample, tip material, and cantilever spring constant, the AC testing voltage used had amplitudes between 0.5 V and 5 V and frequencies between 900 Hz and 75 kHz.

The internal source of a Keithley 6517 electrometer was utilized to apply DC bias voltages to the ferroelectric sample. The output voltage resolution of 5 mV when operating in the 100 V range, and the maximum output current of 10 mA were perfectly suited for the poling experiments performed during this work [74]. The lock-in amplifier, the AC source and the DC voltage source were all fully controlled by a computer via an IEEE 488 general

* Connections indicated by the manufacturer.

purpose interface bus, using adequate programs developed in house using the data acquisition and analysis software TESTPOINT (Capital Equipment Corp.).

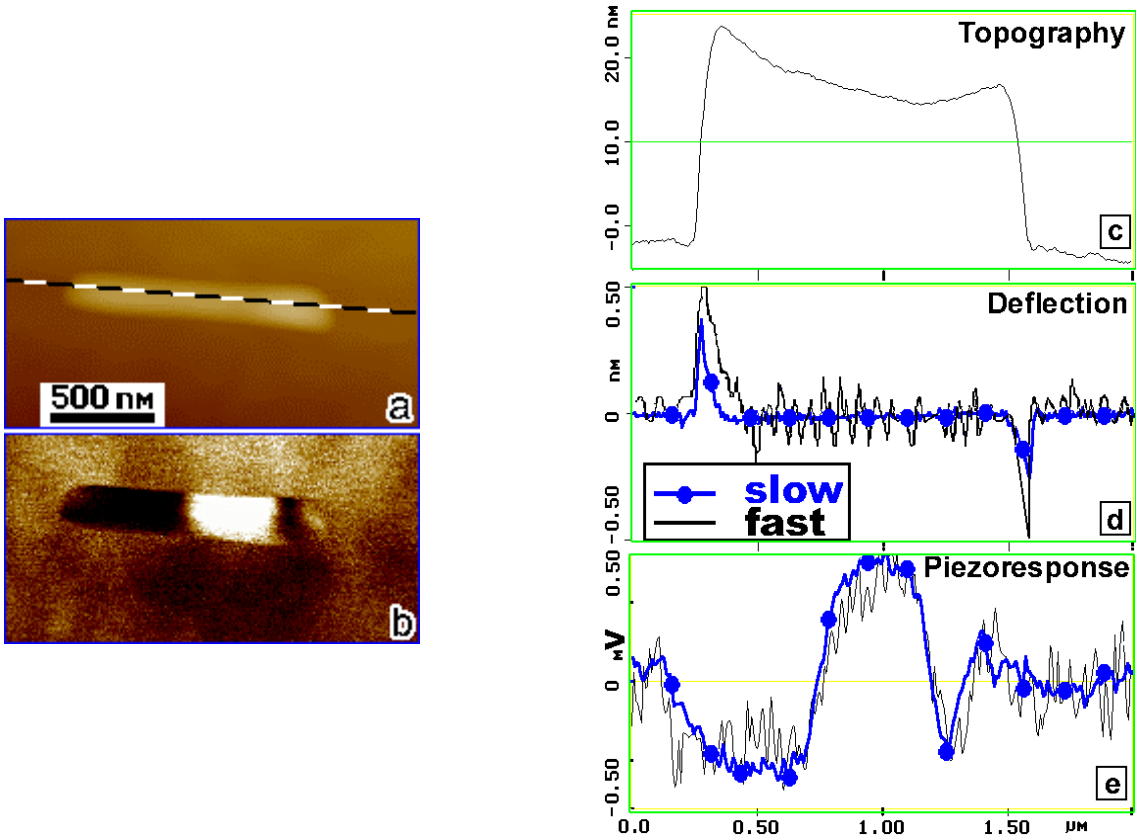

Figure 11 The signals involved in piezoresponse imaging. (a) Topographic image (the height signal) of a $Bi_4Ti_3O_{12}$ grain (the black-white dashed line has been added). (b) The domain structure (z-piezoresponse signal). (c–e) The height (c), the vertical deflection (d), and the piezoresponse (e) signals along the dashed line in (a). The lines with dots in (d) and (e) were acquired with a much lower scan speed than that used for the measurement of the thinner lines.

The most important component of the SFM setup is the SFM tip, which senses the sample surface. Different types of SFM probes were used in this work.

Silicon nitride cantilevers are the standard for contact mode AFM measurements, because this material is hard to wear, works well with most of the samples, allows the use of a very low contact force between the tip and the sample surface (less than 10 nN), and they are rather cheap. However, they need a conductive coating for use in electric force microscopy, in particular for piezoresponse measurements. Difficulties with metal coating of silicon nitride[**] prevented their exclusive use in these measurements. In general, the silicon nitride probes are suited for low-contact-force piezoresponse imaging [57], but not for the quantitative ferroelectric characterization of the films.

Highly doped silicon cantilevers with a resistivity of 0.02 Ωcm have spring constants between $4\,N/m$ and $50\,N/m$ depending on the cantilever geometry [75]. The forces on the

[**] Soft cantilevers easily bend when coated. Stress control of the coating requires a very special equipment. The tip sharpness also deteriorates considerably. Moreover, the conductive layer may be removed at the tip apex after several scans, causing a drastic deterioration of the piezoresponse images.

sample can be derived from the spring constants and they were between 0.05 μN and 10 μN. These SFM probes were mostly used in the present work due to the following reasons:

- The high doping level with boron acceptors assures a good electrical conductivity of the probe, without any metal coating. The quality of the electrical contact remains constant during the whole experiment, even if the apex geometry changes during the scanning.
- A high spring constant of the cantilever means a high mechanical resonance frequency, which allows the use of a high frequency for the AC testing voltage.
- For piezoelectric measurements in atomic force microscopy, it was proved that the effects of the electrostatic interaction between the tip-cantilever and sample-bottom electrode systems are highly reduced [76] by using cantilevers with high elastic constant.

The lower limit for the lateral resolution achieved is directly related to the radius of the tip apex, and it was estimated to be about 10 nm – 20 nm for the soft cantilevers, and 30 nm – 50 nm for the stiff cantilevers.

All experiments described in this work were done under ambient conditions, at room temperature.

3.4 Investigated systems

3.4.1 Epitaxial thin films

Epitaxial ferroelectric thin films of $SrBi_2Ta_2O_9$ (SBT), $Bi_4Ti_3O_{12}$, and $BaBi_4Ti_4O_{15}$ were deposited by pulsed laser deposition (PLD) onto epitaxial layers of electrically conductive $LaNiO_3$. The epitaxial $LaNiO_3$ layer served both as a template favoring the epitaxial growth of the ferroelectric film and as a bottom electrode for the electrical characterization. The conductive $LaNiO_3$ epitaxial layers were grown either on top of *(100)*-oriented $SrTiO_3$ (STO) single crystals or on top of *(100)*-oriented single-crystalline silicon substrates previously coated with a stack of epitaxial CeO_2 and YSZ buffer layers. The CeO_2/YSZ bilayer serves as a template to promote the epitaxial growth of the $LaNiO_3$ electrode layer on Si(100), the $LaNiO_3$ layer promoting the epitaxial growth of the desired bismuth-layered perovskite film [77,78].

All the films and layers were grown by PLD employing a KrF excimer laser ($\lambda = 248\,nm$) at a laser repetition rate of 5 or 10 Hz. The depositions of all the films were performed in a pure oxygen atmosphere in a continuous sequence without breaking the controlled atmosphere conditions. The films were grown on substrates heated at high temperatures estimated to lie between 675°C and 685°C for YSZ and between 650°C and 670°C for the other materials. After the deposition of the bismuth-layered perovskite film the epitaxial heterostructure was slowly cooled down to room temperature in 13.3 Pa of pure oxygen. The deposition parameters used, as well as the typical thickness obtained for the different deposited materials, are summarized in Table 1.

The structure of the films was studied by X-ray diffraction (XRD) using a Philips X'Pert MRD four-circle diffractometer and plan-view and cross-section TEM. The morphology of the films consists of a c-oriented matrix with embedded grains of another orientation. The detailed XRD analysis of all the bismuth-layered thin films showed that the

grains have *(110)$_{orth}$* and *(100)$_{orth}$* orientations and are embedded into the *(001)*-oriented (i.e. *c*-oriented) film matrix [79]. This observation is fully consistent with the SFM and TEM investigations as shown in Figure 12.

Deposition parameters	YSZ	CeO_2	$LaNiO_3$	$Bi_4Ti_3O_{12}$	SBT	$BaBi_4Ti_4O_{15}$
Repetition rate (Hz)	10	10	5	10	10	10
Pulse energy (mJ)	450	350	350	350	350	350
Energy density (J/cm^2) (on the target)	3	2.7	2.7	2.7	2.7	2.7
Heater temperature (°C)	820	800	800	800	800	800
Substrate temperature (°C) (estimated)	680	665	665	665	665	665
Oxygen pressure (x7.5 Pa)	10^{-2}	100	300	100	100	100
Film thickness (nm)	≈50	≈20	≈50	≈400	≈150	≈300

Table 1 Summary of the deposition conditions used for the growth of epitaxial YSZ, CeO_2, $LaNiO_3$, $Bi_4Ti_3O_{12}$, SBT, and $BaBi_4Ti_4O_{15}$ films.

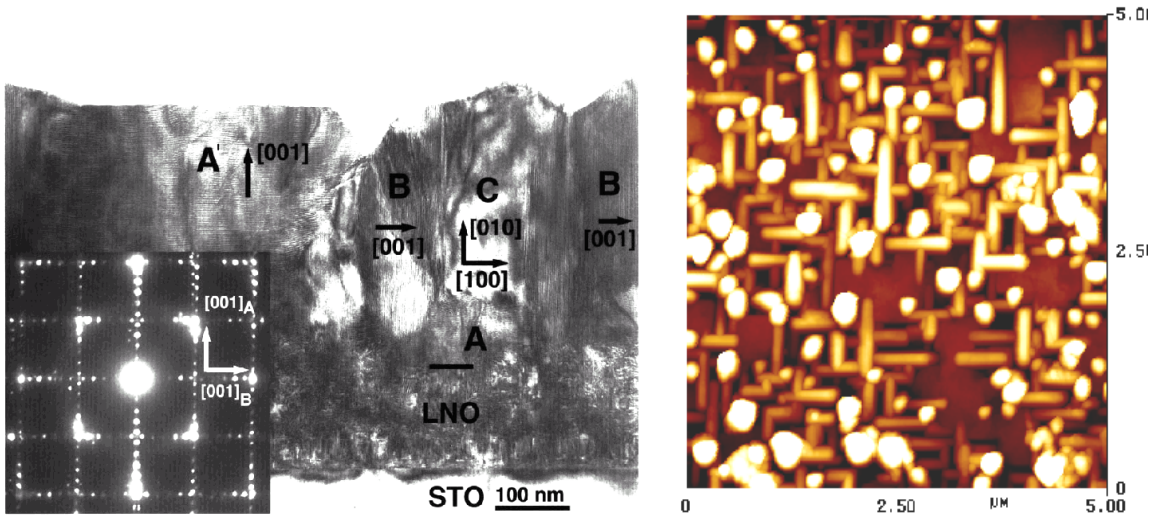

(a) **(b)**

Figure 12 Typical characteristics of the epitaxial films (here $BaBi_4Ti_4O_{15}/LaNiO_3$/ STO): **(a)** cross section TEM image of rectangular-shaped crystallites. The image shows the *c*-oriented grains (A, A') and also the *(110)$_{orth}$*-oriented grains (B and C). The inset displays a selected area diffraction pattern corresponding to both *(001)*–and *(110)$_{orth}$*-oriented regions. **(b)** SFM topography image of a region similar to that of (a). Note that tetragonal indexing is used in (a), so that, e.g., $[010]_t = [110]_{orth}$.

3.4.2 Polycrystalline PZT films

PZT thin films were deposited using the chemical solution deposition (CSD) method. The PZT precursor solution was prepared with Pb acetate, Ti- and Zr-isopropylate as metal precursor, and with 2-methoxyethanol (2ME) as solvent. Pb acetate was dissolved in 2ME, dehydrated at 125°C and then cooled to about 80°C. Separately, Ti and Zr isopropylate were dissolved in 2ME and the solutions were heated up to 125°C under stirring to evaporate water and any reaction by-products. The Ti and Zr solutions were stabilized against hydrolysis by reaction with acetylacetonate. After cooling down to 80°C, Pb, Ti and Zr precursor solutions were mixed and the final solution was heated to 120°C under continuous stirring and kept under these conditions until a concentration of about 0.1 mol^{-1} was achieved. After cooling down to room temperature, the obtained PZT precursor solution was filtered with a 0.22 μm teflon filter.

The PZT thin films were obtained by solution spinning onto the substrates at 2000 rpm for 35 s. The metalorganic films were dried at 120°C for 1 min. and successively pyrolised on a hot plate at 300°C for 5 min. For the specific concentration (of the solution) used, the thickness of one coating was about 150 nm. The spinning-pyrolysing sequence was repeated several times to increase the film thickness to the desired value. Finally the PZT films were crystallized by conventional thermal annealing for 30-60 min. performed in air at temperatures ranging from 550°C to 650°C.

3.4.3 Patterned nanostructures

Regular $SrBi_2Ta_2O_9$ (SBT) and PZT structures with lateral sizes under 100 nm were fabricated using electron beam direct writing (EBDW) [80]. Electron beam lithography is one of the next-generation lithography processes allowing a resolution down to several tens of nanometers,. EBDW is a maskless lithography process widely used for writing metallic and oxide nanostructures using metalorganic precursors [81] and alleviates the etching of the ferroelectric thin film, which is known to be an unsolved problem at these dimensions [82]. Chemical reactions are locally induced in a metalorganic thin film by irradiation with an electron beam having sufficient energy and dose and the desired pattern is written by scanning the electron beam over the sample. The pattern is developed by dissolving the unexposed area in a specific solvent and further transformed into metal or oxide by thermal annealing [83,84].

Test patterns of SBT and PZT cells with lateral dimensions between 1 and 0.125 μm were exposed into a corresponding metalorganic film using a commercial electron beam lithography system (ELPHY Plus) adapted to a JEOL JSM 6400 scanning electron microscope (SEM) working at an acceleration voltage of 40 kV. Exposure was performed at electron doses varying from 1500 to 6000 $\mu C/cm^2$ for PZT and 600 to 1200 $\mu C/cm^2$ for SBT. The structures were developed by immersing the exposed sample for 1 min. in toluene, and were then dried by blowing with nitrogen.

After developing, the metalorganic mesas were subsequently transformed into an oxide by annealing in air for 5 min. at 300 °C and further crystallized into the ferroelectric phase by annealing at temperatures ranging from 600 to 850 °C.

Representative structures consisting of periodic patterns of ferroelectric cells yielding a memory density of 1 $Gbit/cm^2$ are presented in Figure 13. The cells are well defined in shape

and are polycrystalline with grains having sizes of 20 nm or less (smaller for PZT than for SBT). During the crystallization process, the smallest SBT structures lose their rectangular shape while PZT structures maintain their shape even after a 50% shrinkage.

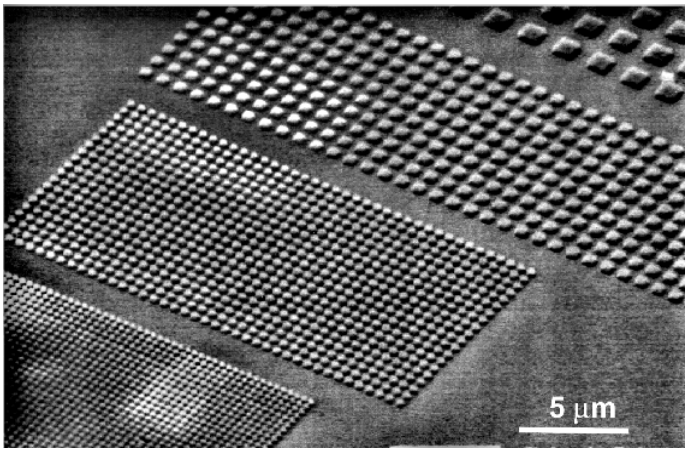

Figure 13 Metalorganic SBT test structures developed in toluene after e-beam exposure with an electron dose of 3 $\mu C/cm^2$.